

# Dual Functional Eudragit® S100/L30D-55 and PLGA Colon-Targeted Nanoparticles of Iridoid Glycoside for Improved Treatment of Induced Ulcerative Colitis

This article was published in the following Dove Press journal:  
International Journal of Nanomedicine

Chenzhe Gao,<sup>1,2,\*</sup> Shen Yu,<sup>2,\*</sup>  
Xiaonan Zhang,<sup>3</sup> Yanxin Dang,<sup>2,4</sup>  
Dan-dan Han,<sup>2</sup> Xin Liu,<sup>2,5</sup>  
Janchun Han,<sup>1</sup> Mizhou Hui<sup>1</sup>

<sup>1</sup>Food Science College, Northeast Agricultural University, Harbin, People's Republic of China; <sup>2</sup>Department of Pharmaceutical Engineering, School of Materials Science and Chemical Engineering, Key Laboratory of Green Chemical Engineering in Heilongjiang Province, Harbin University of Science and Technology, Harbin, People's Republic of China; <sup>3</sup>College of Biological and Food Engineering, Guangdong University of Petrochemical Technology, Maoming, People's Republic of China; <sup>4</sup>Pharmacy Department, Fourth Affiliated Hospital, Heilongjiang University of Chinese Medicine, Harbin, People's Republic of China; <sup>5</sup>Department of Pharmacology, School of Medicine, Yale University, New Haven, Connecticut, USA

\*These authors contributed equally to this work

Correspondence: Xin Liu  
Department of Pharmaceutical Engineering,  
School of Materials Science and Chemical  
Engineering, Key Laboratory of Green  
Chemical Engineering in Heilongjiang  
Province, Harbin University of Science and  
Technology, Harbin, 150040, People's  
Republic of China  
Tel +86 451-86392728  
Fax +86 451-86392710  
Email xinliu98@126.com

Janchun Han  
Food Science College, Northeast  
Agricultural University, Harbin, 150030,  
People's Republic of China  
Tel/Fax +86 451-55190716  
Email hanjanchun@neau.edu.cn

**Aim:** Iridoid glycosides (IG) as the major active fraction of *Syringa oblata* Lindl. has a proven anti-inflammatory effect for ulcerative colitis (UC). However, its current commercial formulations are hampered by low bioavailability and unable to reach inflamed colon. To overcome the limitation, dual functional IG-loaded nanoparticles (DFNPs) were prepared to increase the residence time of IG in colon. The protective mechanism of DFNPs on DSS-induced colonic injury was evaluated in rats.

**Materials and Methods:** We prepared DFNPs using the oil-in-water emulsion method. PLGA was selected as sustained-release polymer, and ES100 and EL30D-55 as pH-responsive polymers. The morphology and size distribution of NPs were measured by SEM and DLS technique. To evaluate colon targeting of DFNPs, DiR, was encapsulated as a fluorescent probe into NPs. Fluorescent distribution of NPs were investigated. The therapeutic potential and in vivo transportation of NPs in gastrointestinal tract were evaluated in a colitis model.

**Results:** SEM images and zeta data indicated the successful preparation of DFNPs. This formulation exhibited high loading capacity. Drug release results suggested DFNPs released less than 20% at the first 6 h in simulated gastric fluid (pH1.2) and simulated small intestine fluid (pH6.8). A high amount of 84.7% sustained release from NPs in simulated colonic fluid (pH7.4) was beyond 24 h. DiR-loaded NPs demonstrated a much higher colon accumulation, suggesting effective targeting due to functionalization with pH and time-dependent polymers. DFNPs could significantly ameliorate the colonic damage by reducing DAI, macroscopic score, histological damage and cell apoptosis. Our results also proved that the potent anti-inflammatory effect of DFNPs is contributed by decrease of NADPH, gene expression of *COX-2* and *MMP-9* and the production of TNF- $\alpha$ , IL-17, IL-23 and PGE2.

**Conclusion:** We confirm that DFNPs exert protective effects through inhibiting the inflammatory response, which could be developed as a potential colon-targeted system.

**Keywords:** iridoid glycoside, ulcerative colitis, *Syringa oblata* Lindl., pH-sensitive and time-dependent, colon-targeted nanoparticles

## Introduction

Ulcerative colitis (UC) is a chronic inflammatory disorder of the rectum and colon.<sup>1</sup> The incidence of UC is increasing during the past three decades worldwide, which may progress to colorectal cancer.<sup>2</sup> The symptoms of UC range from diarrhea, fecal blood and weight loss to ulceration and complete obstruction of the gastrointestinal

tract (GIT), which can negatively affect daily life of patients.<sup>3,4</sup> However, the therapeutic effect of many currently marketed formulations (tablets and capsules) remain unsatisfactory for its clinical treatment, most often due to their low oral bioavailability attributed to the lack of targeted delivery of drugs specifically to the inflamed colon tissue.<sup>5</sup> After administration, the entire drug is rapidly released in the stomach and small intestine, and most of the drug is absorbed into the blood circulation. Consequently, the systemic drug concentration resulted in related side effects and lower drug concentration in the inflamed colon, which led to poor therapeutic efficacies. Therefore, it is essential to develop an innovative strategy to specifically delivery therapeutic agents to the inflamed colon for a prolonged period in a sustained manner while improving oral bioavailability and reducing the risk of systemic adverse effects.<sup>6</sup>

Iridoid glycosides (IG), the main bioactive fraction isolated from the leaves of *Syringa oblata* Lindl. is a Chinese medicine ingredient traditionally used for treatment of inflammatory bowel disease (IBD).<sup>7,8</sup> Our previous studies have reported the protective effects of IG on UC because of its anti-inflammatory, anti-apoptotic, anti-oxidative and immunomodulatory properties.<sup>2,9</sup> The capsules and tablets of IG have been developed in Drug Standard by Ministry of Health of People's Republic of China (PRC).<sup>4</sup> Despite the role of IG in chemotherapy, the beneficial effect of IG on colonic tissue is constrained by its conventional oral formulations due to the nonspecific drug release in the upper GIT and rapid metabolism,<sup>10</sup> which lead to low oral bioavailability of IG. The therapeutic goal of drug delivery in colitis therapy is to deliver the maximum amount of drug to the inflamed colon while minimizing systemic drug absorption and unwanted side effects in the early parts of the GIT.<sup>11</sup> Hence, it is urgent to develop a high-loading colon-targeted formulation for IG that can improve its oral bioavailability and prolong its retention in colon.

In recent years, the development of colon-targeted oral nanoparticles (NPs) have been paid more attention as a powerful tool to deliver therapeutic agents for the treatment of UC owing to their ability to selectively accumulate in inflamed colonic mucosa.<sup>12</sup> Several studies have demonstrated that colon-targeted local drug delivery approach can improve local drug concentration, reduce dosage and minimize systemic drug absorption to avoid adverse effects.<sup>13,14</sup> In addition, colon-targeted oral NPs exhibit size-dependent adhesion to inflamed tissues of the

colon, enhance the systemic bioavailability of poor absorbed drugs as the long retention time in colon in experimental UC.<sup>15,16</sup> In this study, we prepared dual-functional IG-loaded colon-targeted oral polymeric NPs using poly (lactide-co-glycolide) (PLGA) as a sustained-release polymer, as well as EL30D55 and ES100 as a combination of pH-sensitive polymers to overcome the limitations of single-triggered release systems. PLGA copolymers were approved by the FDA for numerous applications, including controlled-release NPs for colon targeting.<sup>17</sup> It has been proven that the time required for the degradation of PLGA is associated to the ratio of monomers used in its production, ie, controlling the degradation rate can be achieved by adjusting the ratio of DL-lactide to glycolide in the copolymer.<sup>18</sup> EL30D55 and ES100 are proven to be biocompatible enteric polymers for oral formulations.<sup>19,20</sup> The enteric polymers EL30D-55 usually used as outer coating layer for oral formulations can prevent the drug release in gastric acidic conditions, and then manipulate the drug release within the desired pH range of 5.5~7.0 in the distal small intestine.<sup>21</sup> ES100 is a pH-sensitive methacrylate copolymer that dissolves above pH 7.<sup>22</sup> The appropriate colon dissolution pH of delivery system can be controlled by optimizing the ratio of EL30D55 and ES100 for targeted drug delivery to the inflamed colon and thus improve the therapeutic efficacy of the drug. The objectives of this combination of dual-functional IG-loaded colon-targeted oral polymeric NPs were to minimize early drug release in the stomach and small intestine, to obtain sustained drug release throughout the colon, and to target the inflamed colonic mucosa.

UC is a chronic intestinal inflammation with complex pathogenesis, which was triggered by numerous inflammatory mediators and cytokines.<sup>2,23</sup> In the inflammatory process, lots of inflammatory mediators and cytokines, such as NADPH oxidases (NOXs), cyclooxygenase (COX)-2, matrix metalloprotein-9 (MMP-9), tumor necrosis factor- $\alpha$  (TNF- $\alpha$ ), interleukin 17 (IL-17) and IL-23 involved in the immune response.<sup>24,25</sup> Oxidative stress has been identified as a major factor that contributes to the pathogenesis and progression of IBD, and NADPH oxidases (NOXs) are the main sources of ROS.<sup>2</sup> Growing evidence suggests that there is a positive correlation between upregulated NADPH oxidase (NOX) expression and gastrointestinal inflammation.<sup>26</sup> Prostaglandin E2 (PGE2) is also another important inflammatory mediator produced from arachidonic acid metabolites catalyzed by COX-2 in inflammatory responses.<sup>27</sup>

In current work, the pH/time dependent dual-functional IG-loaded NPs intended for inflamed colon targeted-drug delivery in UC were prepared using the oil-in-water emulsion solvent evaporation method. For comparison, single pH-dependent NPs and time-dependent NPs were also prepared. The physicochemical properties of the dual-functional NPs were characterized, and their therapeutic efficacy was evaluated and compared in mouse model of dextran sulfate sodium (DSS)-induced colitis. Furthermore, oral pharmacokinetics, live images and organ fluorescent distribution studies were performed in rats to confirm the colonic release of drug. To investigate the protective mechanism of dual-functional IG-loaded NPs on DSS-induced colonic mucosal injury, the production of TNF- $\alpha$ , IL-17, IL-23 and PGE2 in colon mucosa were detected by enzyme-linked immunosorbent assay (ELISA). The activity of NADPH was also evaluated. The mRNA and expressions of *COX-2* and *MMP-9* were measured by real-time quantitative PCR, respectively.

## Materials and Methods

### Materials

Iridoid glycosides (IG) were extracted from the leaves of *Syringa oblata* Lindl., and purified by macroporous resin under the guidance of our previously established procedure.<sup>2</sup> PLGA (DL-lactide/Glycolide 50:50 copolymer) was synthesized by solid phase polycondensation reaction as our previous work.<sup>28</sup> Methacrylic acid copolymers, EL30D-55 and ES100 were supplied by Röhm GmbH (Darmstadt, Germany). Methanol (HPLC grade) was purchased from Sigma Aldrich (St. Louis, MO, USA). Dextran sulfate sodium (DSS, molecular weight 36~50 kDa) was provided by MP Biomedicals (Irvine, California (CA), USA). TdT-mediated dUTP nick end labeling (TUNEL) cell apoptosis detection kit was obtained from Roche Systems, Inc. (Basel, Switzerland). The cytokine enzyme-linked immunosorbent assay (ELISA) kits were supplied by R&D Systems (Minneapolis, MN, USA). The primers for real-time PCR were synthesized by Invitrogen Biological Engineering Technology & Services Co., Ltd. (Beijing, China). All other reagents were the highest analytical grade commercially available.

### Animals

Sprague-Dawley (SD) rats (male, 200~220 g) and imprinting control region (ICR) mice (male, 20~25 g) were

provided by the Center of Experimental Animals of Harbin Medical University (Harbin, China). All animals were housed at least 1 week to adapt to the new environment with a temperature of  $22 \pm 1^\circ\text{C}$  and a relative humidity of  $65\% \pm 5\%$  under a 12 h light/dark cycle. Animal experiments were approved by the Institutional Animal Care and Use Committee of Northeast Agricultural University under the approved protocol number SRM-06 in accordance with the guidelines followed for the welfare and ethics of the laboratory animals of Northeast Agricultural University (NEAUEC20200402).

### Preparation of IG-Loaded NPs

The pH/Time dependent dual-functional IG-loaded NPs were prepared by an oil-in-water emulsion/solvent evaporation method with some modifications.<sup>11</sup> The single pH-sensitive NPs and time-dependent NPs were also prepared for comparison. Briefly, for the formulation of pH-sensitive NPs, ES100 (12% w/v) was dissolved in 1 mol/L  $\text{NH}_4\text{OH}$  and homogenized for about 1h to form a homogenous polymer solution. Then, ES100 dispersion was filled into EL30D-55 dispersion (30% w/v) under continuous stirring to form a pH-sensitive polymer mixture. The pH-sensitive polymer mixture (100 mg) was dissolved with IG (10 mg) in 3 mL of acetone/methanol solvent mixture (1: 2 v/v). This solution was slowly injected using a syringe pump at a flow rate of 0.5 mL/min into 40 mL of 0.25% w/v polyvinyl alcohol-124 (PVA-124) solution with 500 rpm stirring.

IG-loaded time-dependent NPs were prepared via the optimized emulsion/solvent evaporation method according to our previous reports.<sup>28</sup> Briefly, 100 mg PLGA and 10 mg IG were dissolved in 3 mL dichloromethane, and then 1 mL of 0.25% PVA-124 aqueous solution was added drop-wise. The mixture was then emulsified by sonication (200 w) under the conditions of ultrasound 10 s, intermittent 10 s with a Digital Control Ultrasonic Instrument (KQ5200-DB, Kunshan Ultrasonic Instrument Co. Ltd, China) for 10 min in an ice water bath. The emulsion was immediately poured into 30 mL of stirring 0.5% PVA-124 solution for 20 min under magnetic stirring and dichloromethane was eliminated by evaporation under magnetic stirring for 4 h. The resulting IG-loaded time-dependent NPs suspension was purified by centrifugation (15,000 rpm, 10 min) using an AvantiJXN-30 centrifuge (Beckman Counter, California (CA), USA) at  $4^\circ\text{C}$ . Thereafter, IG-loaded time-dependent NPs were

resuspended and washed with ultra-pure water to remove excess PVA-124.

For the preparation of pH/Time dependent delivery system, IG-loaded dual-functional NPs were prepared with PLGA and pH-sensitive polymer mixture (1:1 w/w) using the oil-in-water emulsion/solvent evaporation method. Briefly, PLGA (50 mg) and pH-sensitive polymer dispersion (EL30D-55 and ES100, 50 mg) was dissolved in 3 mL dichloromethane with IG (10 mg). This organic mixture was then emulsified in 10 mL acidic PVA-124 solution (0.5% w/v) using an ultrasound probe sonicator (200 w, 5 min) in an ice bath. This emulsion was then diluted with 50 mL of acidic PVA-124 solution (0.25% w/v). The organic solvent was evaporated at room temperature for 6 h in a fume hood under magnetic stirring. After evaporating the residual solvent, the NPs were collected by centrifugation (15,000 rpm for 30 min), and washed with deionized water 3 times. The pH/Time dependent dual-functional NPs were collected for further analysis.

## Physicochemical Characterization of NPs

The morphology of IG-loaded dual-functional NPs was analyzed by a scanning electron microscope (SEM, SUPRA 55 SAPPHERE, ZEISS, Germany). The particle size, size distribution and polydispersity index (PDI) zeta potential of this Nano drug delivery system were measured using a Nano ZS90 Zetasizer (Malvern Zetasizer, Malvern Instruments, Malvern, UK) based on the dynamic light scattering (DLS) technique.

IG entrapped in the dual-functional NPs was evaluated using high-performance liquid chromatography (HPLC) according to our previously established method.<sup>2,4</sup> The HPLC system used for IG analysis was an UltiMates 3000 DGLC dual three element liquid chromatographic system (Thermo Fisher Scientific, Waltham, Massachusetts, USA) with a reverse-phase Waters C18 column (250 mm×4.6 mm, 5 µm). The mobile phase consisted of methanol and 0.2% (v/v) orthophosphoric acid solution (40: 60, v/v) and the flow rate was set at 1.0 mL·min<sup>-1</sup>. Diode array detection ultraviolet (DAD: UV) maximum absorbance was at 221 nm. The column temperature was maintained at 25°C. The drug loading efficiency (LE) and encapsulation efficiency (EE) of IG-loaded dual-functional NPs were calculated using the following equations:

$$LE\% = M1 - M2/M3 * 100\% \quad (1)$$

$$EE\% = M1 - M2/M4 * 100\% \quad (2)$$

Where  $M_1$  is the total amount of IG entrapped into the dual-functional NPs;  $M_2$  is the free unloaded IG in ES100/EL30D-55 and PLGA suspension;  $M_3$  is total amount of IG-loaded dual-functional NPs;  $M_4$  is total amount of free IG.

## In vitro Drug Release Study

In vitro drug release of IG from the dual-functional NPs was initiated in a phosphate buffer system with gradually changing pH values and general transit time corresponding to the normal variations along the gastrointestinal tract (GIT), ie, form stomach (pH1.2, 0~2h), upper small intestine (pH6.8, 2~6h), and both ileum and colon (pH7.4, 6~24h), respectively.<sup>11,13</sup> Briefly, cumulative IG release from dual-functional NPs was determined by dispersing 1 mg/mL of the drug-loaded NPs in 0.01 M phosphate buffer, and incubating it in a shaking water bath (60 rpm, 37°C). 0.2% Polysorbate 80 (w/v) was added to phosphate buffer to facilitate the solubilization of IG. Aliquots of the dispersion were withdrawn at 0 min, 15 min, 30 min, 1 h, 2 h, 4 h, 6 h, 8 h, 10 h, 12 h and 24 h, and centrifuged at 15,000 rpm for 25 min. Volume of the dispersion withdrawn was replaced with fresh phosphate buffer. The supernatant was collected and the concentrations of IG were analyzed by HPLC. The experiments were performed in triplicates.

## Pharmacokinetics and Organ Distribution Analysis

Pharmacokinetic characteristics of IG-loaded dual-functional NPs were evaluated in SD rats with free IG suspended in 0.5% sodium CMC as control. Briefly, the rats were randomly divided into two groups (n = 10) receiving the same dose of IG (30 mg/kg) in two different formulations p.o., respectively. At each time point, 0.5 mL blood sample was collected and centrifuged (3000 rpm, 10 min) to obtain the plasma. IG in the plasma were then extracted by addition of 1mL acetonitrile. The mixture was vortex-mixed for 1 min followed by centrifugation at 12,000 rpm for 10 min. The supernatant was evaporated under protection of nitrogen and then re-dissolved in 200 µL mobile phase before HPLC-MS analysis. The pharmacokinetic parameters were calculated from the plasma concentrations of IG by linear trapezoidal rule and compared between free drug and the dual-functional NPs using DAS 2.1 software system. The pharmacokinetic



parameters we calculated include maximum plasma concentration ( $C_{\max}$ ), maximum plasma time ( $T_{\max}$ ), the area under the plasma concentration-time curve ( $AUC_{0-48h}$ ) and mean residence time (MRT).

Next, we investigated the biodistribution of IG-loaded dual-functional NPs (DFNPs) in stomach, small intestine and colon to further evaluate its potential as a drug delivery system. Free drug, IG-loaded pH-sensitive NPs (PNPs) and IG-loaded time-dependent NPs (TNPs) were used as controls. Briefly, SD rats were randomly divided into four groups ( $n = 5$ ), each group was given a single dose of 30 mg/kg free IG and the other two formulations by intragastric administration, respectively. Animals were sacrificed at 24 h and 48 h after oral administration. Then, the entire GI tract was excised and segmented into stomach, small intestine, and colon. The mesenteric and fatty tissues were separated. Blood was cleared prior to organ distribution study. Stomach, small intestine, and colon were weighed and homogenized, respectively. The homogenate was centrifuged at 6000 rpm for 15 min at 4°C and supernatants were collected. The amount of drug distributed in unit mass of stomach, small intestine and colonic tissue were determined by HPLC at 24 h and 48 h, respectively.

## Induction of DSS-Mediated Colitis

Acute colitis in male ICR mice and male SD rats were induced using a dose of 4% (w/v) DSS in drinking water ad libitum for 7 days, respectively.<sup>2,13</sup> After induction of colitis, the administration of DSS was stopped and replaced with tap water. Mean DSS water consumption, body weight, and development of clinical symptoms of colitis, such as diarrhea and rectal bleeding, were assessed daily during the colitis induction period.<sup>11</sup>

## Distribution of NPs in the GIT of Mice with DSS-Induced Colitis

To evaluate specific colon targeting of the dual-functional NPs after UC, the same procedure was followed for the preparation of fluorescent loaded dual-functional NPs. IG was replaced by the fluorescent marker DiR to facilitate in vivo analysis of the distribution and localization of the dual-functional NPs in the GIT of ICR mice with DSS-induced colitis.<sup>13</sup> DiR-loaded dual-functional NPs were prepared by dispersing blank dual-functional NPs (10 mg) in PBS buffer (3 mL, 0.1 M, pH = 7.0). DiR fluorescent dye (1 mg) solubilized in 0.1 mL dimethyl

sulphoxide (DMSO) was then added to the buffer. The solution was stirred overnight in the dark at room temperature. After reaction, the mixture was centrifuged (6000 rpm, 10 min) 4 times.

For live imaging studies, ICR mice with DSS-induced colitis were orally administrated with DiR-loaded dual-functional NPs at a dose of 5 mg·kg<sup>-1</sup>. In vivo distribution of dual-functional NPs was evaluated using a BRUKER IS4000MM PRO image station system (BioSpin, BrukerCorporation, Billerica, MA, USA) 6 h and 12 h after administration. Associated default conditions for fluorescence imaging: exposure time = 2 s and the camera was set to an f-stop = 2. Filter setting: excitation (470 nm)-emission (0 nm).

## Evaluation of in vivo Therapeutic Efficacy

SD rats were randomly divided into 5 groups ( $n = 6$ ). (I) Normal control group: mice received 0.9% saline only; by contrast, (II) Model group (colitis control): rats with DSS-induced colitis treated with blank dual-functional NPs; (III) IG-loaded pH-sensitive NPs (PNPs) treatment group; (IV) IG-loaded time-dependent NPs (TNPs) treatment group; and (V) IG-loaded dual-functional NPs (DFNPs) treatment group. Rats were orally treated with IG-loaded different NPs at a dose of IG 30 mg/kg once for 14 days after administration of DSS.

In the experimental period, weights of rats were recorded daily. The colitis severity was evaluated daily using a disease activity index (DAI) consisting of three parameters: weight loss, stool consistency, and anal bleeding, as described previously.<sup>9,29</sup> Macroscopic damage was assessed based on the previously established scoring system.<sup>4</sup>

## Histological Study of Colitis by H&E Staining

The therapeutic potential of colon-targeted IG-loaded dual-functional NPs for UC was also supported by histological examination of the colon tissues from all treatment groups. Therefore, rats were sacrificed, and the colon tissue was excised at the termination of the experiment. The colon tissues were fixed in 4% paraformaldehyde, then embedded in paraffin, and finally sectioned in 4 µm sections. The samples were stained with hematoxylin and eosin (H&E) according to the standard procedures for histological evaluation.<sup>2,4</sup> Microscopic examination of prepared slides was performed to analyze pathomorphological changes in

the mucosal, sub mucosal, muscular and serosal layers of colon specimen. The histological damage scores were assessed based on the previously established scoring system.<sup>2</sup>

## Apoptosis Assay

The colonic cell apoptosis was assessed using the terminal deoxynucleotidyl transferase- (TdT-) mediated dUTP-biotin nick end labelling (TUNEL) kit. TUNEL-positive epithelial cells in colonic tissue were clearly identified as brown-stained nuclei, which suggested DNA fragmentation due to apoptosis. TUNEL-positive expression was detected via 1000 cells in random fields.

## Assessment of the Activity of NADPH Oxidase

The activity of NADPH oxidase was detected as previously reported.<sup>2</sup> In brief, colon samples were homogenized in 10 volumes of 0.1M Tris-HCl buffers (pH7.4) using an electric homogenizer (IKA T10, Germany) in an ice bath. The homogenate was centrifuged at 10,000 rpm at 4°C for 30 min and obtained the supernatant. 20 µL supernatant of homogenized and centrifuged brain samples was added into a 96-well luminescence plate, then mixed with 80 µL phosphate-buffered saline and 6.25 µL 1 M lucigenin. NADPH was added to start the reaction, and photoemission was determined by the absorbance at 340 nm, which is monitored every 30 s for 5 min.

## Determination of Proinflammatory Cytokine

The colon tissues were homogenized in ice-cold physiological saline at the final concentration of 10% (w/v). Proinflammatory cytokine levels of TNF-α, IL-17, IL-23 and PGE2 in colon tissue homogenates (1/5 dilution) were detected using ELISA Kits (Nanjing Jiancheng Biological Engineering Institute, Jiangsu, China) following the manufacturer's protocol.

## Immunohistochemical Staining of Colon Tissues

The protein expressions of *COX-2* and *MMP-9* were quantified according to a method described previously.<sup>2,9</sup> Briefly, 4 µm colon sections were first treated with 3% hydrogen peroxidase for 10 min to block endogenous peroxidase, then incubated with the polyclonal primary antibody of COX-2 and MMP-9 (diluted to 1: 100) overnight at 4°C. The colon sections were then washed with phosphate-buffered saline (PBS) and incubated with polyclonal rabbit anti-mouse biotinylated secondary antibody (Dako, CA, USA). After that, colon sections were incubated with 3, 3'-diaminobenzidine solution (Sigma-Aldrich, St. Louis, MO, USA) and then stained with hematoxylin. Finally, images were observed under an Olympus BH-2 microscope (Tokyo, Japan).

## Real-Time PCR

Colon tissues were homogenized in a lysis buffer for RNA isolation. Total RNA isolation from colonic cells was performed using the TRIzol reagent (Invitrogen, Carlsbad, CA, USA) according to the manufacturer's manual. RNA was transcribed into cDNA using the first-strand cDNA synthesis kit (Fermentas International Inc., Burlington, Canada) in accordance with the manufacturer's instructions. The primer sequences for real-time PCR analysis are shown in Table 1. mRNA expressions were normalized to *GAPDH* (18 S rRNA endogenous control) and calculated according to the  $2^{-\Delta\Delta Ct}$  method (n = 6).

## Statistical Analysis

All the experimental data are presented as mean ± standard deviation (Mean ± SD). ANOVA (Design Expert version 7.0.0) was used to evaluate the significance in differences among results. One-way ANOVA with post hoc test was applied to the in vivo therapeutic study. Statistical analysis

**Table 1** Sequences of the Amplification Primers Used in the Real-Time PCR

mRNA Species		Oligonucleotides (5'→3')	Product Size (bp)
COX-2	Forward	ACTACGCCGAGATTCCTGACA	584
	Reverse	ACTGATGAGTGAAGTGCTGGG	
MMP-9	Forward	GCAAACCCTGCGTATTTCCATT	283
	Reverse	GCGATAACCATCCGAGCGAC	
GAPDH	Forward	TTCCTACCCCCAATGTATCCG	270
	Reverse	CCACCCTGTTGCTGTAGCCATA	

was performed with SPSS 19.0 statistical software. *P*-values < 0.05 were considered to be a statistically significant difference.

## Results

### Characterization of Dual-Functional NPs

In the current study, SEM morphology images indicated the successful preparation of IG-loaded dual-functional NPs with regularly spherical shape and a smooth surface (Figure 1A). Further, dynamic light scattering (DLS) also revealed the homogeneous nanosize distribution of IG-loaded dual-functional NPs with average diameter equal to  $247 \pm 26$  nm (Figure 1B) and a low polydispersity index (PDI) ( $0.21 \pm 0.05$ ). The zeta potential of IG-loaded dual-functional NPs was determined to be  $-22.4 \pm 1.76$  mV. The drug loading capacity (LC%) and encapsulation efficiency (EE%) of IG-loaded dual-functional NPs are  $12.77 \pm 0.51\%$  and  $39.47 \pm 2.69\%$ , respectively.

### In vitro Drug Release and Particle Size at Different pH Values

In order to investigate the release behavior of IG from DFNPs, the release profiles of IG from different NPs were determined in gradually pH-changing simulated medium (pH 1.2, 6.8, and 7.4), which resemble the pH values of the stomach, the upper part of the small intestine, and ileum/colon, respectively (Figure 2A). As expected, no significant difference in drug release behavior were observed between

PNPs and DFNPs at the stomach pH (pH 1.2) and small intestine pH (pH 6.8), with less than 20% of the IG released during the first 6 h. However, TNPs showed sustained release and its release rate was not affected by pH changes in the simulated release medium. Compared with the other two nanoformulations, TNPs exhibited a burst drug-release profile in the first 6 h because of the pH independent characteristics of PLGA. Approximately 70% of IG was released from TNPs in simulated gastric fluid (pH 1.2) and simulated small intestine fluid (pH 6.8). The premature drug release of TNPs would lead to absorption in the small intestine, which resulted in unwanted side effects and insufficient drug delivery to the inflamed colon. The release behavior of TNPs demonstrated that single time-dependent NPs are not suitable for colon delivery.

Apparently, PNPs and DFNPs showed remarkably different release profiles at the ileum/colon pH (pH 7.4). PNPs showed a sudden burst release (nearly 100%) of IG, owing to the complete dissolution of pH-sensitive polymers (ES100 and EL30D-55) at  $\text{pH} > 7$ . The release behavior of PNPs indicated that the single pH-dependent nano formulation would not be suitable for colon-specific delivery because of the burst drug release in the ileum. In contrast, DFNPs can avoid complete drug release at pH 7.4 and show sustained drug release properties. These results confirmed that pH/Time-dependent DFNPs can efficiently retain the entrapped drug until reaching the colon, improving the bioavailability of drug in the colon, which is a potential nanoformulation for colon-targeted delivery.

The particle size of three respective NPs at different pH values agree with their release behaviors (Figure 2B). All NPs exhibited no size changes at pH 1.2 and 6.8. Specially, PNP particles were not observed at pH 7.4, indicating complete dissolution of the enteric polymers (ES100 and EL30D-55) and the drug release. However, TNPs and DFNPs maintained their intact nanoparticle morphology at pH 7.4 and no significant change in size was detected. In brief, the results of size analysis demonstrated that DFNPs possessed dual characteristics of pH-sensitive and sustained release, while maintaining nanoparticulate morphology. These characteristics of dual-functional nanoformulation are desirable for colon-targeted UC therapy.

## Pharmacokinetics and Biodistribution Study

To evaluate the in vivo performance of IG-loaded dual-functional NPs, the systemic pharmacokinetics in DSS-induced colitis rats were studied with free drug as the

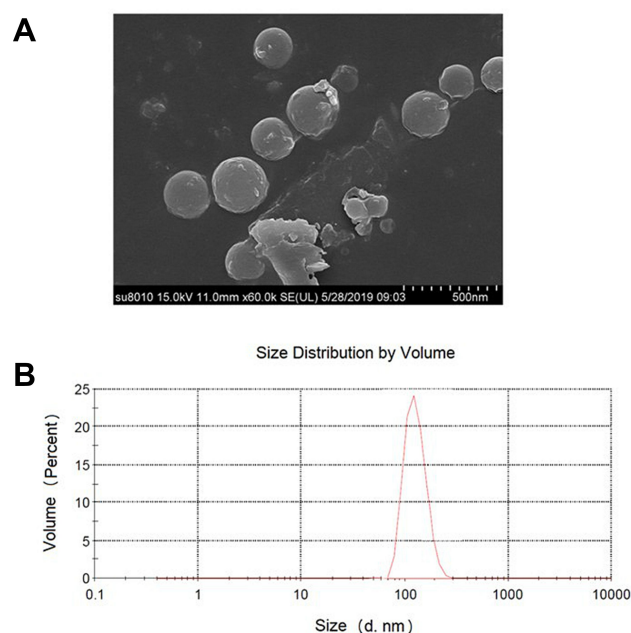


**Figure 1** Morphology and size analysis of IG-loaded dual-functional NPs: (A) SEM images; (B) size histograms.

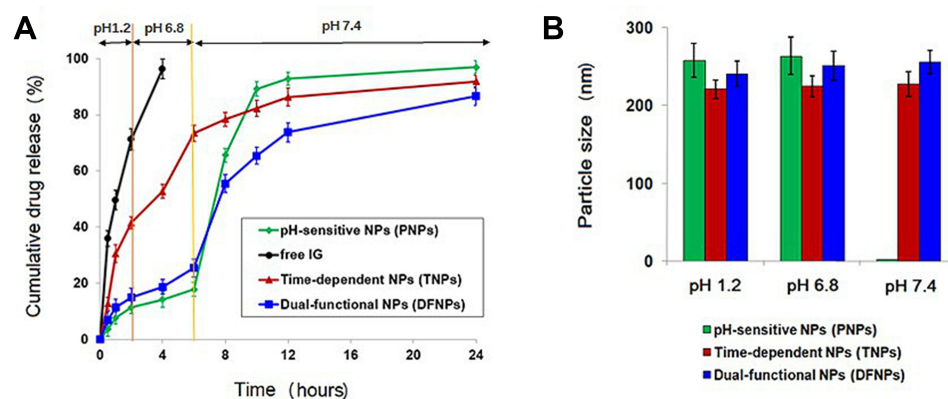


**Figure 2** In vitro drug-release profiles and size analysis of IG-loaded pH-sensitive NPs (PNPs), IG-loaded Time-dependent NPs (TNPs), and IG-loaded dual-functional NPs (DFNPs): (A) in vitro drug release in gradually pH-changing simulated medium; (B) size analysis at different pH values.

control. The pharmacokinetic parameters evaluated are listed in Table 2. The study showed longer  $T_{max}$  value for dual-functional NPs than free IG. However,  $C_{max}$  and  $AUC_{0-48h}$  values were higher in case of free drug than dual-functional NPs. As shown in Figure 3, free IG can not be considered as colon specific because the drug starts appearing in plasma at 40 min after administration ( $0.13 \pm 0.11 \mu\text{g/mL}$ ). Drug concentration was rapidly increased and reached to maximum concentration ( $C_{max} 7.69 \pm 0.46 \mu\text{g/mL}$ ) at 4 h, and then quickly cleared from blood. The higher  $C_{max}$  and  $AUC_{0-48}$  of free IG is due to the absorption of maximum amount of drug from the upper part of GI tract. Notably, Free IG was almost not detectable in plasma at 8 h due to its poor stability and short half-life, which could be easily phagocytosed by the reticuloendothelial system (RES).<sup>10</sup>

In contrast,  $C_{max}$  ( $2.76 \pm 0.27 \mu\text{g/mL}$ ) of IG-loaded dual-functional NPs was measured in plasma at 10 h, since the degradation of pH-sensitive polymers (ES100 and EL30D-55) and time-dependent PLGA by colonic microflora is a slow process that requires several hours for completion. IG-loaded dual-functional NPs exhibited significantly prolonged retention in blood, which could still keep higher drug concentrations in plasma

16 h after oral administration ( $0.32 \mu\text{g/mL}$ ). Especially, the plasma drug concentration of the dual-functional nanoformulation could be detected in plasma even after 20 h ( $0.08 \mu\text{g/mL}$ ).  $AUC_{0-48h}$  and MRT of the dual-functional nanoformulation significantly extended 2.5 times and 3 times compared with free drug, respectively. The longer  $T_{max}$  of the dual-functional NPs indicated that this nanoformulation can prevent drug release in the upper part of the GI tract and releases it in the colon. The lower value of  $C_{max}$  and  $AUC_{0-48}$  of the dual-functional NPs would account for its low systemic bioavailability. Thus, minimal amount of drug is available systemically for interaction with non-target site such that most of the drug resides in the colonic tissue for longer duration for its desired local action at the inflamed colon. The pharmacokinetic parameters prove dual-functional NPs to be efficient colon-target delivery vehicles for IG.

The therapeutic goal of colon-targeted delivery for UC is to deliver the maximum amount of drug to the inflamed colon while minimizing systemic drug absorption and unwanted side effects in the early parts of the GI tract. Therefore, organ distribution study was performed to further confirm the targeting potential of dual-functional NPs by detecting the drug concentration in the stomach, small intestinal and colonic tissues. As shown in Figure 4A, drug concentration was nearly not detected in the stomach at 24 h when rats were administered with free IG while the amount in small intestine and colonic tissues were relatively lower,  $0.28 \pm 0.15 \mu\text{g/g}$  and  $0.09 \pm 0.05 \mu\text{g/g}$ , respectively. The amount of IG in stomach and small intestine tissue from PNPs were obviously higher than TNPs and DFNPs at 24 h, include  $1.49 \pm 0.51 \mu\text{g/g}$  and  $2.23 \pm 0.67 \mu\text{g/g}$ , respectively ( $p < 0.01$ ). Distribution results in the colon indicated that IG

**Table 2** The Main Pharmacokinetic Parameters of IG Following Oral Administration of Free Drug and IG-Loaded Dual-Functional NPs

Pharmacokinetic Parameters	Free IG	IG-Loaded Dual-Functional NPs
$T_{max}$ (h)	$2.51 \pm 0.34$	$10.16 \pm 0.49$
$C_{max}$ ( $\mu\text{g/mL}$ )	$7.69 \pm 0.46$	$2.76 \pm 0.27$
$AUC_{0-48h}$ ( $\mu\text{g/L/h}$ )	$18.26 \pm 3.94$	$7.31 \pm 1.89$
MRT (h)	$12.74 \pm 2.18$	$4.26 \pm 0.78$



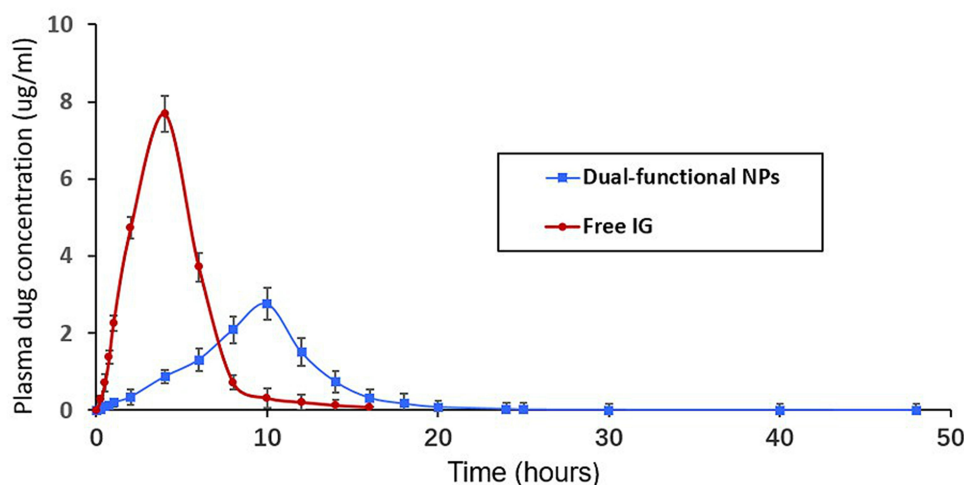


**Figure 3** Plasma concentrations time profile of IG after a single oral dose of free drug and IG-loaded dual-functional NPs.

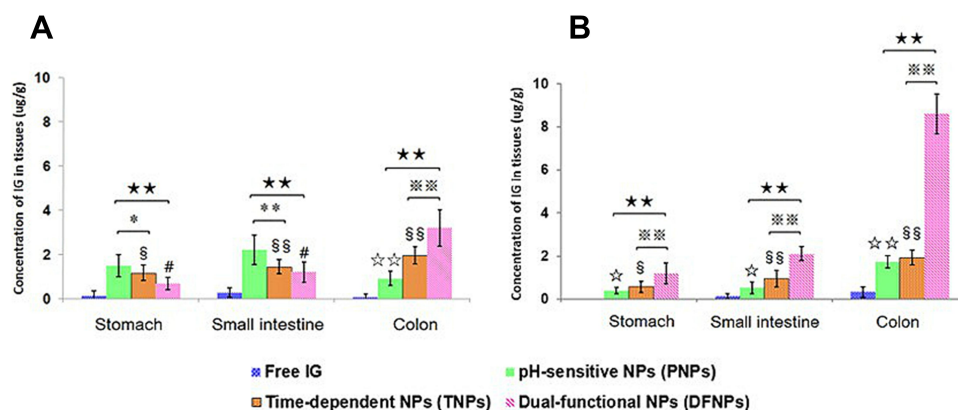


**Figure 4** Distribution of free IG, IG-loaded pH-sensitive NPs (PNPs), IG-loaded time-dependent NPs (TNPs) and IG-loaded dual-functional NPs (DFNPs) in different tissues at 24 h (A) and 48 h (B) post administration.

**Notes:** §  $p < 0.05$ , §§  $p < 0.01$  TNPs vs free IG; ☆  $p < 0.05$ , ☆☆  $p < 0.01$  PNPs vs free IG; #  $p < 0.05$ , DFNPs vs free IG; \*\*  $p < 0.01$  PNPs vs TNPs; \*\*\*  $p < 0.001$  PNPs vs DFNPs; ※  $p < 0.01$  TNPs vs DFNPs.

levels were significantly higher in rats administered DFNPs than administered PNPs or TNPs ( $p < 0.01$ ).

Notably, IG was almost undetectable throughout the GIT at 48 h when given as a free drug. Whereas, treatment with DFNPs, highest drug level ( $8.63 \pm 0.94 \mu\text{g/g}$ ) was detected in colonic tissues at 48 h compared with stomach ( $1.19 \pm 0.48 \mu\text{g/g}$ ) and small intestinal tissue ( $1.01 \pm 1.09 \mu\text{g/g}$ ) (Figure 4B). Thus, highest amount of IG was achieved in the colonic tissue on administration of DFNPs at 24 h and 48 h with minimum determination in stomach and small intestine compared to administration of free drug. Thus, the high amount of IG in the colonic tissue suggests that the DFNPs were intact during transit through the stomach and small intestine which causes minimal drug release in the upper part of the GIT compared to colon. The results of organ distribution proved

that the amount of IG in colonic tissue was increased by 2.7 folds from 24 h to 48 h ( $p < 0.01$ ), thus providing a greater scope for chemoprevention at the local site of inflamed colon due to high tissue retention of drug.

## Evaluation of Targeted Properties of Dual-Functional NPs by in vivo Fluorescence Distribution

Evaluation of the colon-targeted properties of the dual-functional NPs was performed by in vivo fluorescence distribution of fluorescent probe-loaded NPs in the GIT of mice with DSS-induced colitis compared with DiR-loaded pH-sensitive NPs (PNPs) and DiR-loaded time-dependent NPs (TNPs). Briefly, biodistribution of PNPs, TNPs and DiR-loaded dual-functional NPs (DFNPs) along the GIT at

6 h and 12 h post oral administration was analyzed using a BRUKER IS4000MM PRO image station system to investigate the specificity of the NPs to target the colon.

As can be seen in the representative ex vivo biodistribution images (Figure 5A), the fluorescence signals of TNPs accumulated less in all major sections of the GIT (ie, stomach, small intestine, and colon), and the live images of TNPs at the time points of 6 h and 12 h suggested similar trends, respectively (Figure 5B and C). These results demonstrated that maximum fluorescent dye was released in upper GIT (stomach and small intestine), and absorbed systemically before reaching the colon. In contrast, the ex vivo image of PNPs exhibited stronger fluorescence signals in the distal small intestine at 6 h compared with TNPs (Figure 5A,  $p < 0.01$ ), indicating the complete dissolution of the pH-sensitive polymers at pH range 6.8~7.0 and release of the fluorescence probe DiR before reaching the colon. The live images of PNPs at the time points of 6 h and 12 h also

confirmed similar results compared with TNPs (Figure 5B and C,  $p < 0.01$ ), respectively.

However, weaker fluorescence signals of PNPs in ex vivo biodistribution (Figure 5A) and live images (Figure 5B and C) were observed in the colon at all time points compared to DFNPs ( $p < 0.01$ ). This result indicated that the fluorescent dye was absorbed or cleared quickly from the GIT after the dissolution of the enteric PNPs. Impressively, DFNPs showed around 3-fold higher colon accumulation in colitis mice at all time points post-administration compared with PNPs. The relative fluorescence intensity (F/%) of DiR-loaded DFNPs and DiR-loaded PNPs at 6 h post-administration in colon were  $15.76 \pm 4.17$  and  $5.27 \pm 1.32$ , respectively. Quantification fluorescent data of DiR-loaded DFNPs and DiR-loaded PNPs at 12 h post-administration were  $24.52 \pm 7.64$  and  $7.93 \pm 2.86$ , respectively. In addition, DFNPs exhibited dominant fluorescence signals in the colon compared to the signals in the other regions of the GIT (such

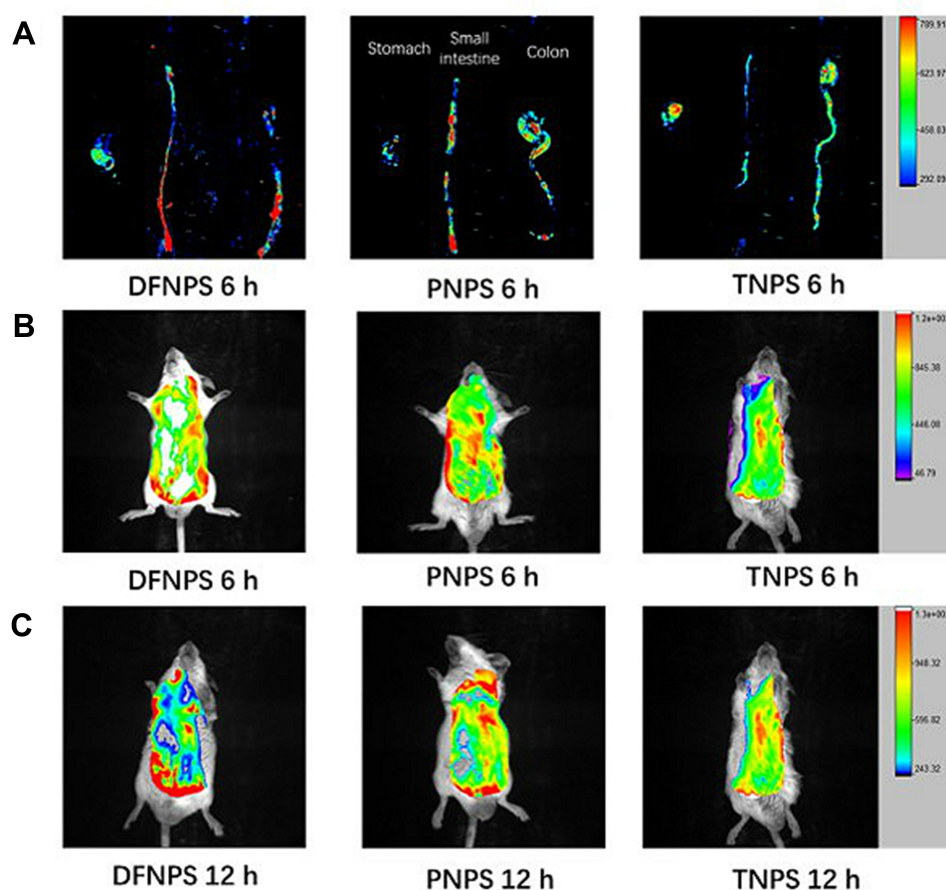


**Figure 5** Representative ex vivo biodistribution of the GIT and live images at 6 h and 12 h after oral administration, evaluating the colon-targeted drug delivery and accumulation potential of DiR-loaded pH-sensitive NPs (PNPs), DiR-loaded time-dependent NPs (TNPs), and DiR-loaded dual-functional NPs (DFNPs), respectively. Ex vivo fluorescence images of organs harvested 6 h (A) after oral administration of DFNPs, PNPs and TNPs, respectively (from left to right). In vivo fluorescence images of animals at 6 h (B) and 12 h (C) after intragastric administration of DFNPs, PNPs and TNPs (from left to right), respectively.

as stomach and small intestine), indicating enhanced drug delivery and maximum targeting accumulation in inflamed colon tissue.

## Therapeutic Efficacy of DFNPs on DSS-Induced Colitis

The sustained drug release profile, favorable pharmacokinetics, and high colon-targeting efficiency of DFNPs make them a promising candidate for further pre-clinical evaluation. We therefore evaluated their therapeutic efficacy in SD rats that with DSS-induced colitis. In this study, DFNPs were orally administrated daily at a dose equivalent to 30 mg IG/kg of IG for a total of 14 days after administration of DSS. PNPs and TNPs were administered in the control groups.

### Macroscopic Injury and Colon Length

Macroscopic analysis of the colon revealed that DSS-induced model group showed significant macroscopic morphological changes, characterized by bowel inflammation, ulceration, bowel wall thickening and necrosis compared with normal control group (Figure 6,  $p < 0.01$ ). In contrast, administration of TNPs attenuated the macroscopic inflammatory injury of acute colitis. Treatment with PNPs markedly suppressed these pathological symptoms (Figure 6) with lower macroscopic score compared with TNPs (Figure 7C,  $p < 0.01$ ). In particular, DFNPs exhibited a better therapeutic effect than single-function NPs (PNPs and TNPs) ( $p < 0.01$ ).

DSS induced a significant shortening of the colon length, which is an index of sufficient induction of colitis and is inversely associated with the severity of colitis.<sup>2,4</sup> As shown in Figure 6, healthy rats usually had an average colon length of  $14.3 \pm 2.2$  cm, while a notable shorten in colon length was observed after induction of DSS-induced colitis (average values of  $5.9 \pm 0.7$  cm). Compared to the DSS-induced colitis group, TNPs treatment obviously reversed the colon shortening ( $8.1 \pm 0.9$  cm,  $p < 0.01$ ), and a significant difference in colon length was observed between TNPs treated rats and DSS colitis rats. Moreover, administration of PNPs markedly improved the colon length shorting compared with TNPs ( $9.8 \pm 1.0$  cm,  $p < 0.01$ ). Remarkably, administration with DFNPs restored colon length to almost  $12.4 \pm 1.3$  cm, which was closer to baseline than other treat groups.

### Body Weight Changes, Macroscopic Score and DAI of Colitis

As shown in Figure 7A, the animals of normal group averagely increased  $14.17 \pm 3.26$  % in the body during the experimental period, whereas a dramatic body weight loss accompanied with obvious diarrhea in model group was observed as the result of DSS-induced acute colitis. In contrast, three groups treated orally with IG-loaded NPs could effectively improve the body weight loss compared with that in the colitis model group ( $p < 0.01$ ). Interestingly, treatment of PNPs could significantly reverse the body weight loss induced by DSS compared to TNPs. Impressively, administration of DFNPs had a faster recovery of body weight loss than those in single-functional NPs group (TNPs and PNPs) ( $p < 0.01$ ). We also evaluated other two important colon mucosa damage index including macroscopic scores and DAI, which were characterized by severe diarrhea, body weight loss, stool consistency, and rectal bleeding.<sup>2,9</sup> The severity of colon injury induced by DSS were shown in Figure 7B and C, model group displayed a significant increase of macroscopic scores and DAI compared to normal group ( $p < 0.01$ ). However, TNPs-treated group could obviously decrease macroscopic scores and DAI compared with colitis control group ( $p < 0.01$ ). In contrast, PNPs could markedly reduce macroscopic scores and DAI compared with TNPs ( $p < 0.01$ ). Especially, DFNPs displayed the most prominent reduction in macroscopic scores and DAI compared to the single-functional NPs (PNPs and ENPs,  $p < 0.01$ ).

### Histological Results

Histological observation results showed that there was no damage on the colon of normal control group (Figure 8A), but the colitis model group displayed serious injury of colonic mucosa ( $p < 0.01$ ). As shown in Figure 8B, DSS administration distorted glandular formation and led to the recruitment of inflammatory cells into the submucosal layer, leading to necrosis, hyperemia, and the superficial epithelium was disruption and exfoliation. In addition, the histologic damage score in the DSS-induced colitis group was higher than that in normal group (Figure 8F,  $p < 0.01$ ). In contrast, treatment with IG-loaded NPs substantially subsided the inflammatory damage of colonic mucosa with lower histologic damage scores (Figure 8C–F,  $p < 0.01$ ). However, histological sections from DFNPs-treated rats demonstrated epithelial restoration and alleviation of inflammation. Histological scores also confirmed the above results, indicating that treatment with DFNPs

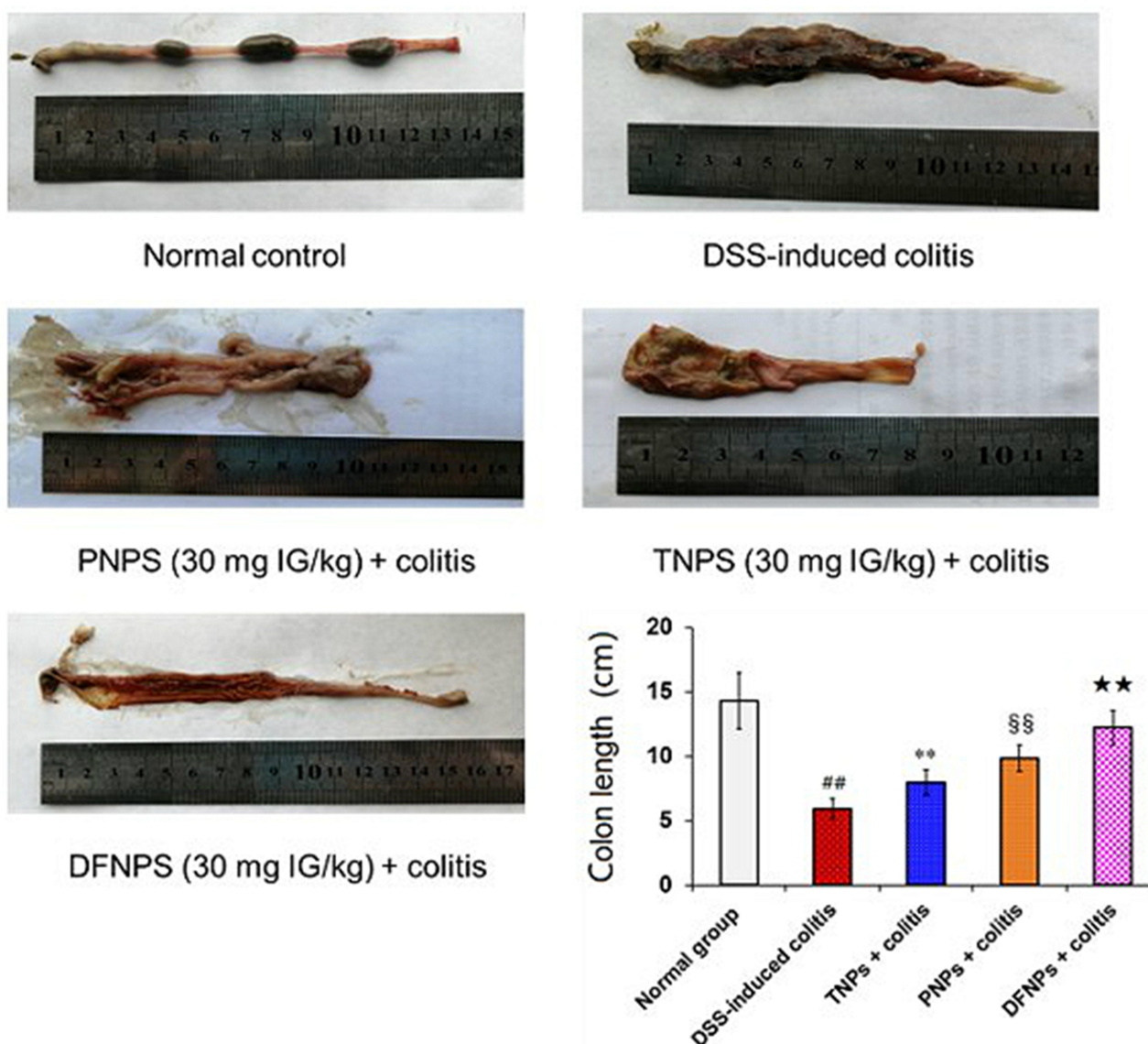


**Figure 6** IG-loaded nanoformulations can attenuate macroscopic injury and colon length shortening in DSS-induced colitis. Representative macroscopic analysis and colon length changes of rat colonic tissues are shown in this figure. Rats were orally treated with different NPs at a doses of 30 mg IG/kg once for 14 days after administration of DSS. Remarkably, IG-loaded dual-functional NPs (DFNPs) significantly attenuated the colon length shortening compared with IG-loaded pH-sensitive NPs (PNPs) and IG-loaded time-dependent NPs (TNPs).

**Notes:** Data are presented as the mean  $\pm$  SD ( $n = 6$  per group). ##  $p < 0.01$  model group vs the normal control group, \*\*  $p < 0.01$  TNPs group vs the DSS-induced colitis group, §§  $p < 0.01$  PNPs group vs TNPs group, and ★★  $p < 0.01$  DFNPs group vs TNPs group.

remarkably attenuated colon inflammation compared to that in the single-functional NPs (TNPs and PNPs, Figure 8C–F,  $p < 0.01$ ). Overall, histological findings demonstrate that DFNPs specially deliver sufficient drug to the inflamed colon, thereby significantly improving the mucosal inflammation of colon.

**Effect of DFNPs on Colonic Epithelial Cell Apoptosis**  
TUNEL assay in the colonic mucosa was performed to investigate the relationship between epithelial cell apoptosis and colitis severity. As shown in Figure 9B and F, TUNEL

staining indicated that DSS ingestion could induce severe colonic mucosal damage compared with the normal group (Figure 9A and F) ( $p < 0.01$ ) by significantly increasing brown apoptotic cells and intercellular apoptotic fragments. IG-loaded single-function NPs may scavenge colonic mucosal damage by inhibiting the elevated levels of colonic apoptosis cells, and there was significant differences between TNPs (Figure 9C) and PNPs (Figure 9D) (Figure 9F,  $p < 0.01$ , compared with model group). Furthermore, DFNPs was the most effective in suppressing intestinal epithelial cell apoptosis (Figure 9E and F). These results further confirm



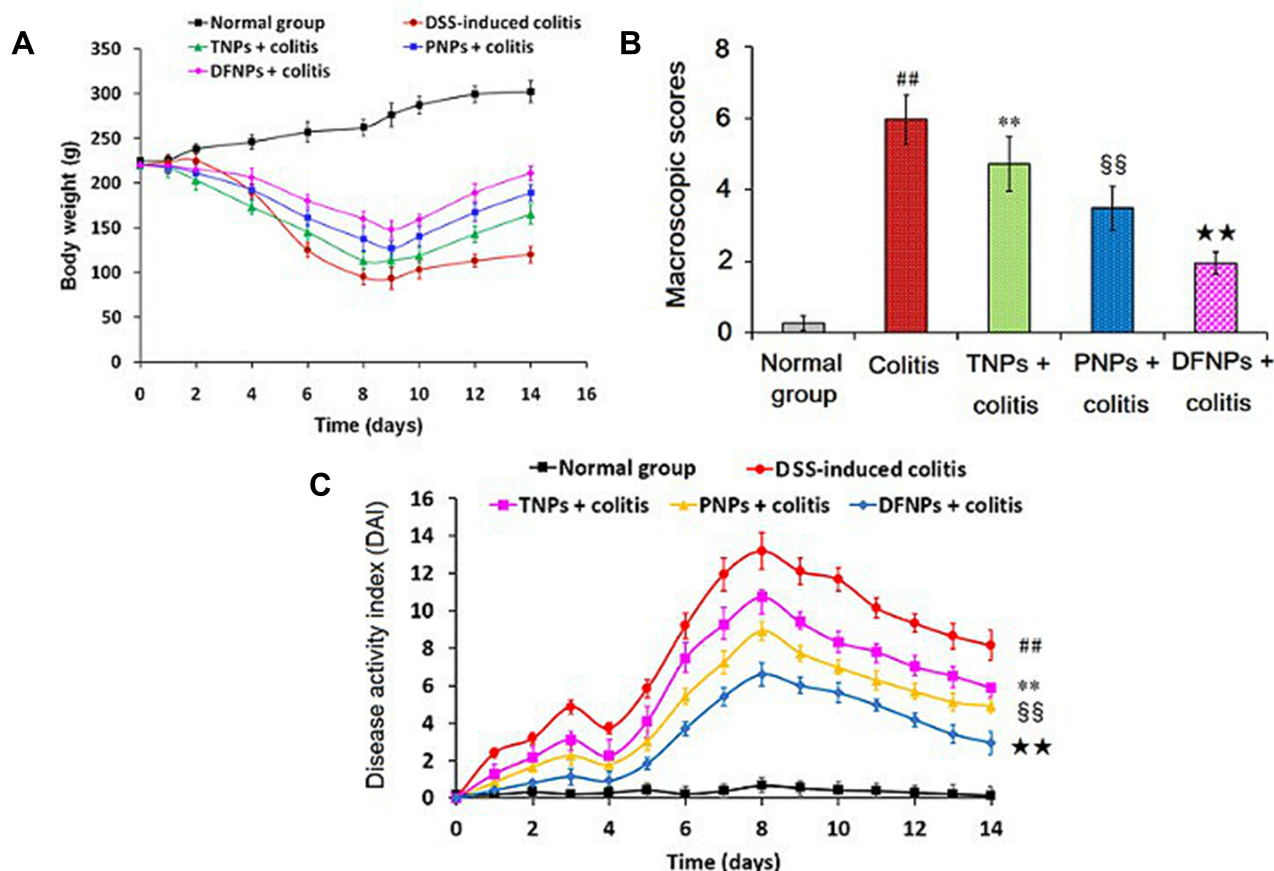


**Figure 7** IG-loaded dual-functional NPs (DFNPs) attenuated the changes in body weight loss (A), macroscopic score (B), and DAI (C) during the experimental period. Rats were orally treated with IG-loaded different NPs at a dose of IG 30 mg/kg once for 14 days after administration of DSS.

**Notes:** Data are presented as the mean  $\pm$  SD ( $n = 6$  per group). ##  $p < 0.01$  vs the normal control group; \*\*  $p < 0.01$  vs the DSS-induced colitis group; §§  $p < 0.01$  vs IG-loaded time-dependent NPs (TNPs) group; ★★  $p < 0.01$  vs IG-loaded pH-sensitive NPs (PNPs) group. Notes:

more efficient drug delivery to the inflamed colon with dual-functional NPs than with PNPs or TNPs for UC therapy.

## Effect of DFNPs on the Activity of NADPH Oxidase and the Production of Pro-Inflammatory Cytokine

In the process of acute inflammation phase of colon, a variety of pro-inflammatory mediators were involved, such as NADPH oxidase, TNF- $\alpha$ , IL-17, IL-23 and PGE2. DSS-induced colitis is associated with elevated NADPH oxidase expression in the colon.<sup>30</sup> Pro-inflammatory cytokines including TNF- $\alpha$ , IL-17 and IL-23 have been considered to play a central role in the processes of UC.<sup>31</sup> PGE2 was increased significantly in patients with IBD, which was important indicator for evaluating the degree of UC.<sup>32</sup> As shown in Figure 10A–E, The activity of NADPH oxidase and the production of pro-inflammatory cytokines (TNF- $\alpha$ , IL-17, IL-23 and PGE2) in the colonic mucosa induced by DSS

was significantly up-regulated compared to normal control group ( $p < 0.01$ ). Treated with IG-loaded single-function NPs could decrease the levels of NADPH oxidase and cytokines in the colonic mucosa compared to model group, and PNPs has more advantage than TNPs in alleviating the elevated free radicals and pro-inflammatory cytokines ( $p < 0.01$ ). Especially, the inhibitory effect of DFNPs on NADPH oxidase and pro-inflammatory cytokines was prior to that of any single-function NPs (PNPs and TNPs,  $p < 0.01$ ).

## Effect of DFNPs on Protein and mRNA Expressions of COX-2 and MMP-9 in DSS-Induced Colitis

Recent studies have demonstrated increased production of COX-2 and MMP-9 in IBD that are known to play a key role in the modulation of intestinal immune system.<sup>25,32</sup> The levels of COX-2 and MMP-9 were increased in IBD and in colon cancer.<sup>33</sup> Therefore, blockade of these inflammatory

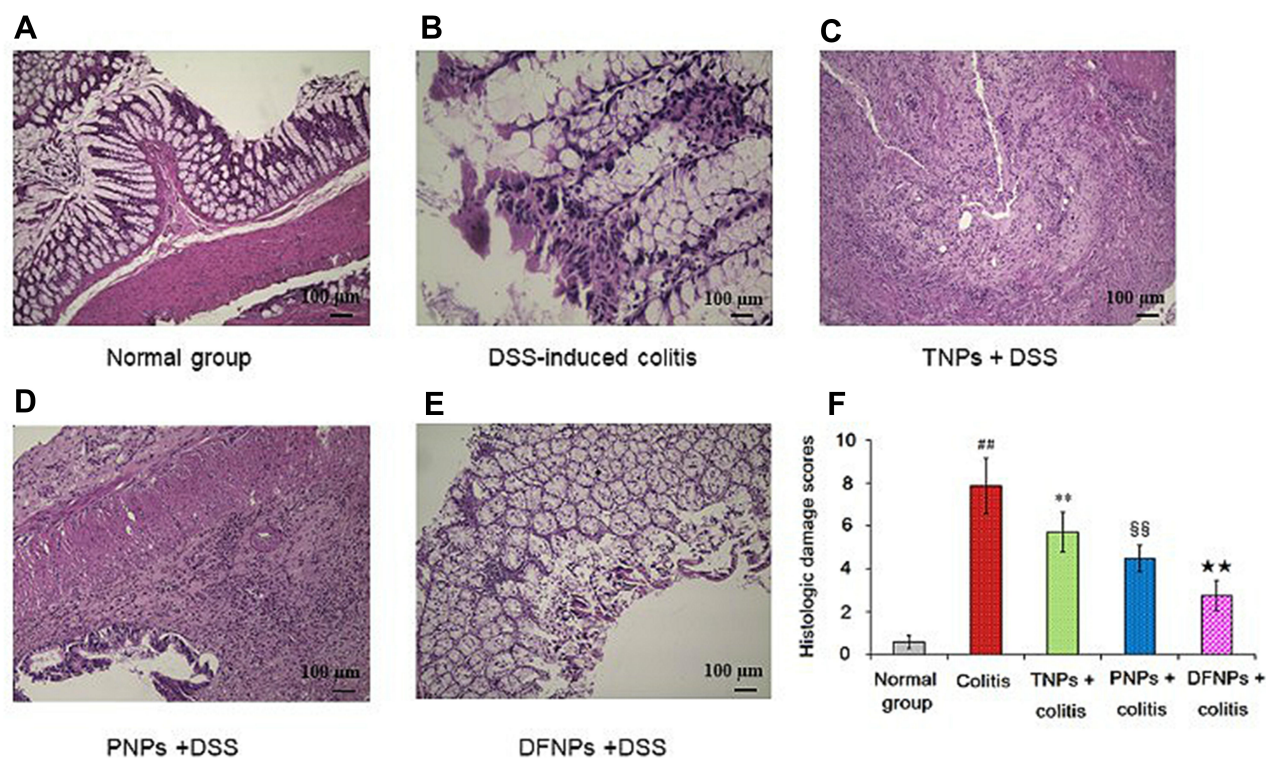


**Figure 8** The protective role of IG-load dual-functional NPs (DFNPs) on DSS-induced histological damage was evaluated by H&E staining (A-F). IG-loaded different NPs were orally administrated at a dose of IG 30 mg/kg once for 14 days after intake of DSS. Histopathological scores of each group were assessed. Colonic tissue sections were observed under a light microscope (100 ×).

**Notes:** Data are presented as the mean  $\pm$  SD ( $n = 6$  per group). ##  $p < 0.01$  vs the normal control group; \*\*  $p < 0.01$  vs the DSS-induced colitis group; §§  $p < 0.01$  vs TNPs + DSS group, and ★★  $p < 0.01$  vs PNPs + DSS group.

mediators can offer an alternative therapy for UC. As it could be informed from Figures 11A and 12A, the mRNA levels of *COX-2* and *MMP-9* in normal group were very low. A significant increase in the protein and mRNA expressions of *COX-2* (Figure 11B and F) and *MMP-9* (Figure 12B and F) were exhibited in colonic epithelia cells of DSS-induced model group ( $p < 0.01$ ). Compared to model group, the protein and mRNA expressions of *COX-2* (Figure 11C, D and F) and *MMP-9* (Figure 12C, D and F) were significantly down-regulated by treating with drug-loaded single-functional NPs (TNPs and PNPs). Furthermore, the effect of PNPs was prior to that of TNPs ( $p < 0.01$ ). The IG-loaded dual-functional NPs exerted the optimum effect in suppressing the protein and mRNA expressions of *COX-2* (Figure 11E and F) and *MMP-9* (Figure 12E and F,  $p < 0.01$ ).

## Conclusion

In the present work, we developed an IG-loaded dual-functional NPs (DFNPs) composed of pH-sensitive biocompatible enteric polymers (EL30D55 and ES100) and time-dependent PLGA polymers for colon targeting delivery and sustained release during UC therapy. The dual-function

nanoformulation presented notable advantages compared with single-function NPs and free drug: (i) avoiding burst drug release in the stomach, thus preventing unwanted side effects; (ii) increasing the residence of drugs in the colon (MRT extended 6.7 times), thereby avoiding drug loss in the upper and middle regions of digestive system; (iii) facilitating the maximum amount of special drug delivery to the inflamed colon (3-fold higher drug accumulation in colon than PNPs and 9-fold higher colon accumulation than free drug) for a prolonged period in a sustained release manner, while improving colon bioavailability.

By comparison, commercially available formulations for UC treatment are not as satisfactory as expected due to the low drug loading capacity, fast metabolic rate and lack of targeted delivery of drugs specifically to the inflamed colon tissue.<sup>5</sup> This dual-ligand nanoformulation with sufficient drug delivery to inflamed colon can provide excellent anti-colitis activity. The next step work we will investigate the safety test of this nanoformulation. The current findings may encourage further researches into the application of dual-targeting nanoformulation for delivery of therapeutic agents for precise therapy of patients with IBD.



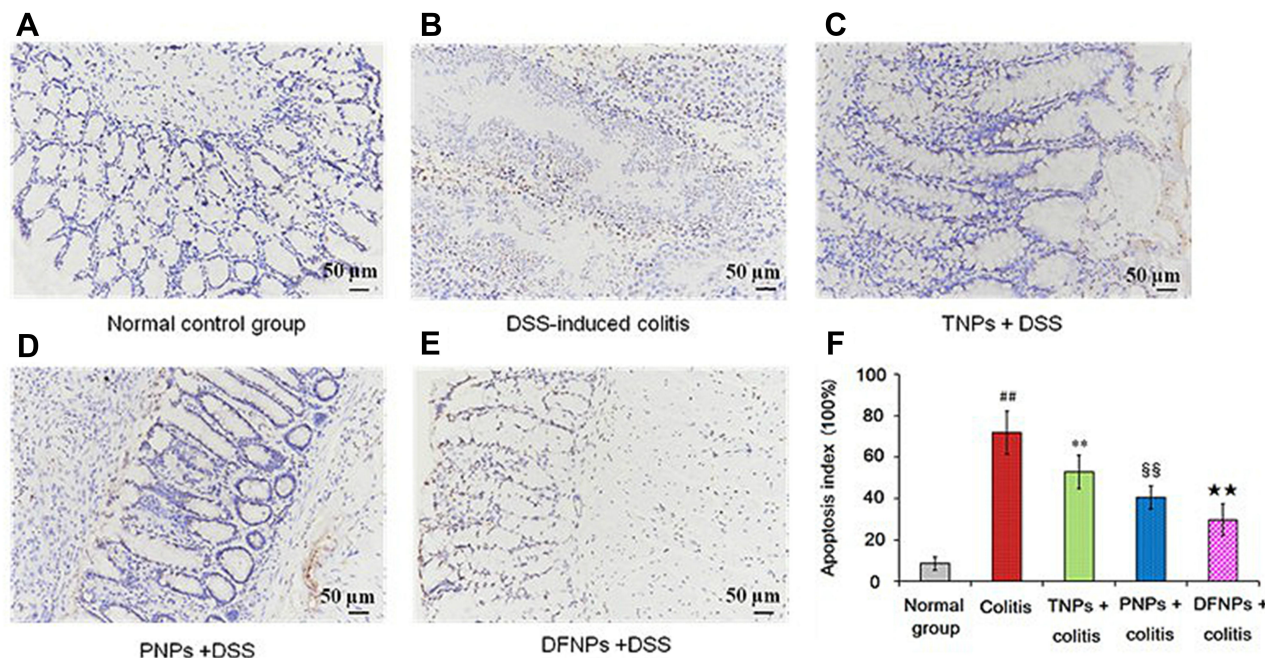


**Figure 9** IG-load dual-functional NPs (DFNPs) attenuated apoptosis in DSS-induced colitis. The effect of different NPs on apoptosis in DSS-induced colitis was assessed by TUNEL staining (A-F). Apoptosis index scores of each group were evaluated.

**Notes:** The scale bar is 50  $\mu$ m. Data are presented as the mean  $\pm$  SD (n = 6 per group). <sup>##</sup> p < 0.01 vs the normal control group; <sup>\*\*</sup> p < 0.01 vs the DSS-induced colitis group; <sup>§§</sup> p < 0.01 vs TNPs + DSS group, and <sup>★★</sup> p < 0.01 vs PNPs + DSS group.

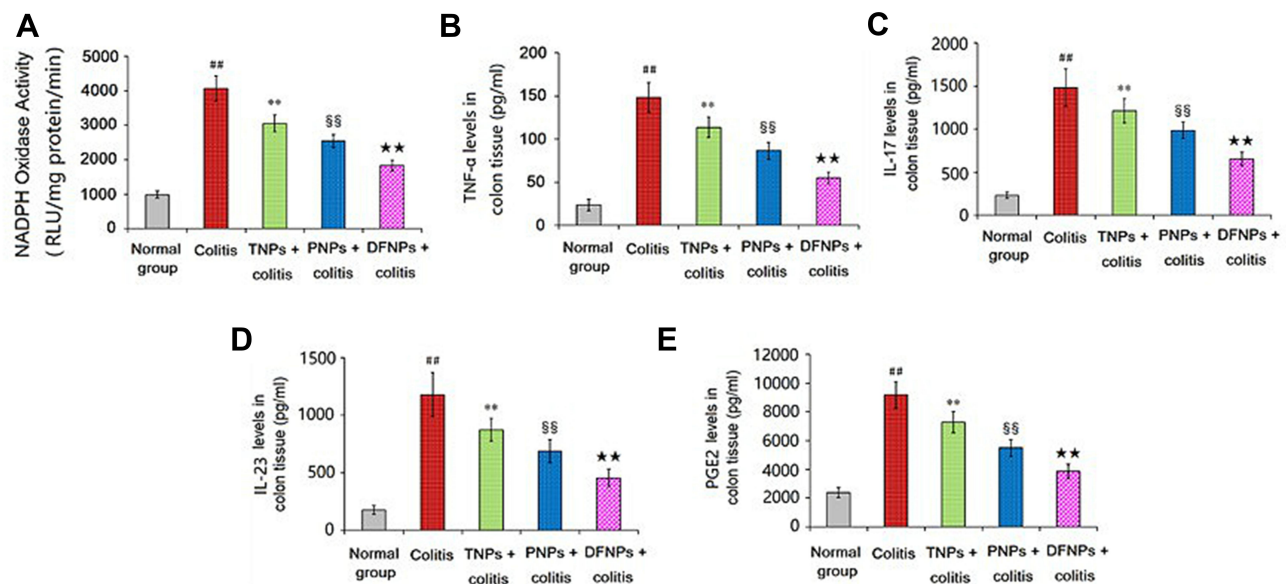


**Figure 10** Effect of IG-load dual-functional NPs (DFNPs) on the activity of NADPH oxidase and the production of TNF- $\alpha$ , IL-17, IL-23 and PGE2 in colonic tissues.

**Notes:** The levels of NADPH oxidase, TNF- $\alpha$ , IL-17, IL-23 and PGE2 were analyzed by commercially available ELISA kits. Data are presented as the mean  $\pm$  SD (n = 6 per group). <sup>##</sup> p < 0.01 vs the normal control group; <sup>\*\*</sup> p < 0.01 vs the DSS-induced colitis group; <sup>§§</sup> p < 0.01 vs TNPs + DSS group, and <sup>★★</sup> p < 0.01 vs PNPs + DSS group.

The results indicated that DFNPs could decrease the colon mucosa damage index by reducing the activity of NADPH oxidase, suppressing the productions of pro-inflammatory cytokines (TNF- $\alpha$ , IL-17, IL-23 and PGE2) and inhibiting gene expressions of inflammatory mediators

(COX-2 and MMP-9). Therefore, current findings will provide strong scientific evidence for the IG-loaded dual-functional NPs to be considered as a new method for special delivery of therapeutic agents to inflamed colon and precise therapy of UC.



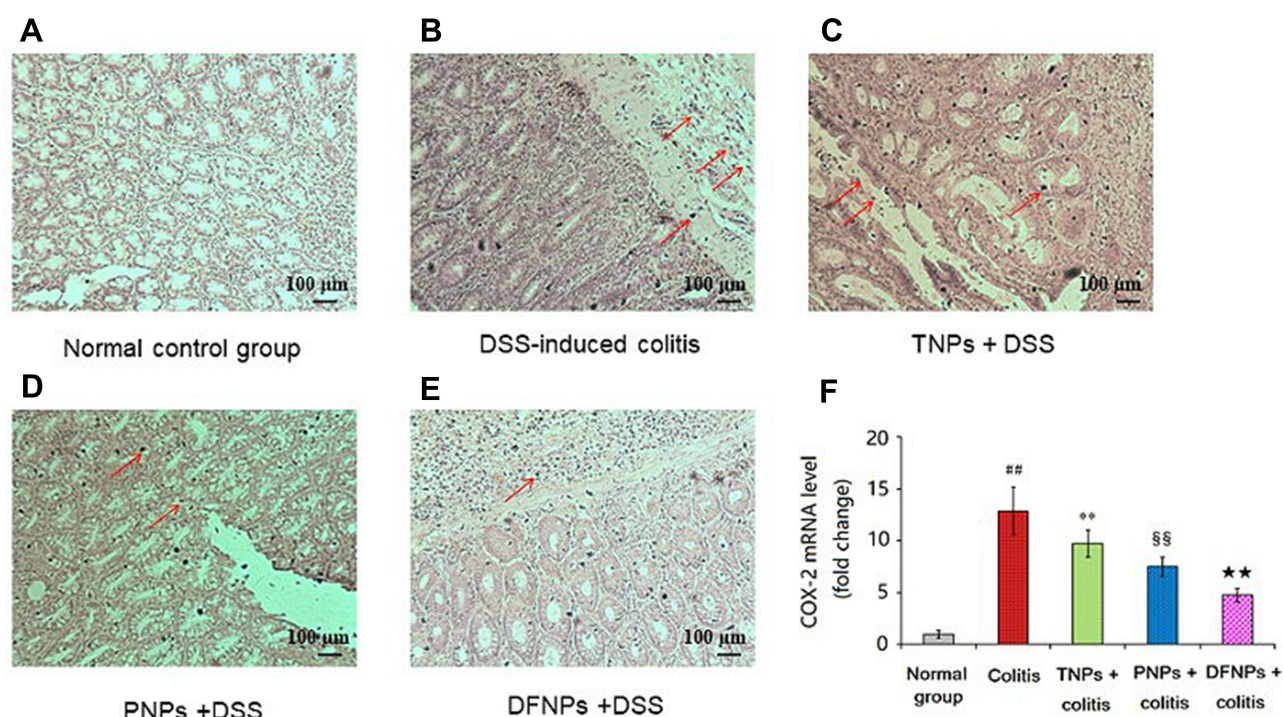


**Figure 11** IG-load dual-functional NPs (DFNPs) reduced mRNA and protein expressions of *COX-2* in DSS-induced colitis (A-F). The protein levels of *COX-2* were analyzed by immunohistochemical staining. The relative mRNA expressions of *COX-2* were normalized to GAPDH.

**Notes:** Data are presented as the mean  $\pm$  SD (n = 6 per group). ## p < 0.01 vs the normal control group; \*\* p < 0.01 vs the DSS-induced colitis group; §§ p < 0.01 vs TNPs + DSS group, and ★★ p < 0.01 vs PNPs + DSS group.

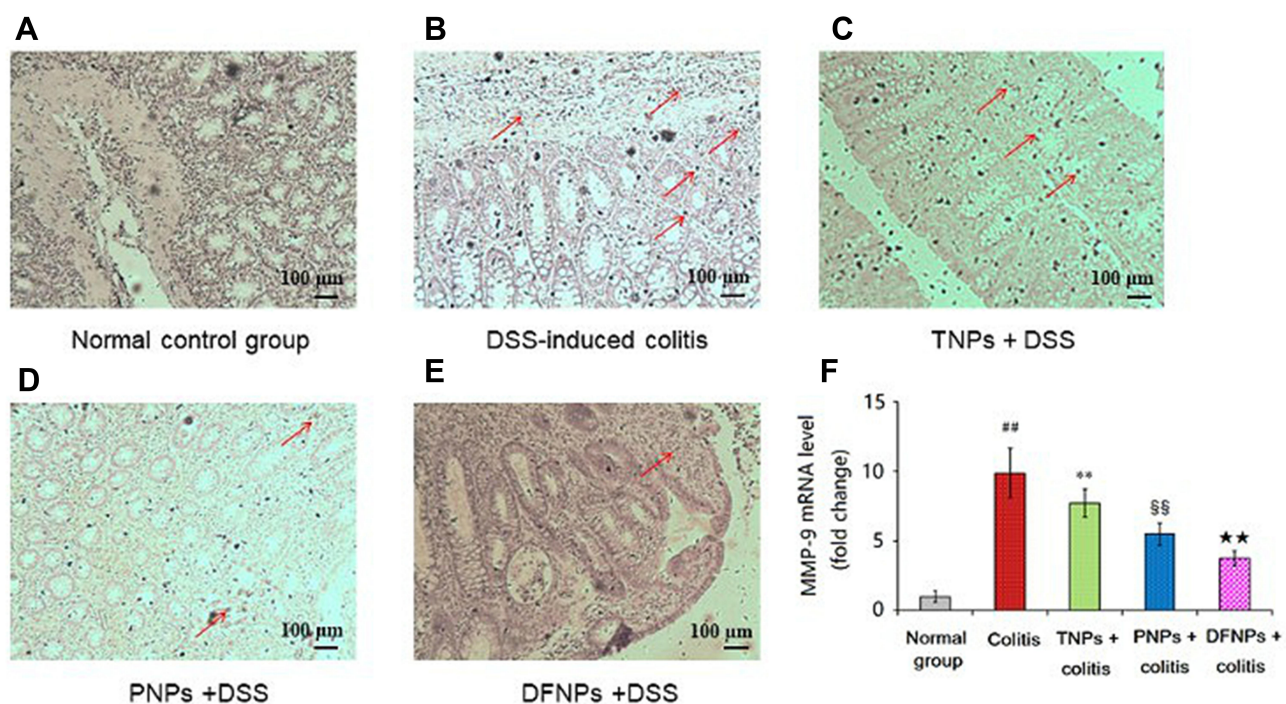


**Figure 12** IG-load dual-functional NPs (DFNPs) reduced mRNA and protein expressions of *MMP-9* in DSS-induced colitis (A-F). The protein levels of *MMP-9* were analyzed by immunohistochemical staining. The relative mRNA expressions of *MMP-9* were normalized to GAPDH.

**Notes:** Data are presented as the mean  $\pm$  SD (n = 6 per group). ## p < 0.01 vs the normal control group; \*\* p < 0.01 vs the DSS-induced colitis group; §§ p < 0.01 vs TNPs + DSS group, and ★★ p < 0.01 vs PNPs + DSS group.



## Abbreviations

UC, ulcerative colitis; IBD, inflammatory bowel disease; GIT, gastrointestinal tract; DSS, dextran sulfate sodium; ES100, Eudragit® S100; EL30D-55, Eudragit® L30D-55; PLGA, poly (lactide-co-glycolide); DiR, 1,1'-diiododecyl-3,3',3'-tetramethylindotricarbocyanine iodide; DMSO, dimethyl sulphoxide; SEM, scanning electron microscopy; PDI, polydispersity index; HPLC, high-performance liquid chromatography; LE, drug loading efficiency; EE, encapsulation efficiency; ICR, imprinting control region; DAI, disease activity index; ELISA, enzyme-linked immunosorbent assay; ANOVA, analysis of variance; TNF- $\alpha$ , tumor necrosis factor- $\alpha$ .

## Acknowledgment

This study was financially supported by the Science and Technology Innovation Program Outstanding Young Talent Project of Harbin, China (Project No. 2016RQYXJ013), the Specialized Research Foundation for the Doctoral Program of Ministry of Education of China (Project No. 20060228005), and Scholarships from the China Scholarship Council (CSC, Project No. 201608930006).

## Disclosure

The authors report no conflicts of interest for this work.

## References

- Travis SP, Danese S, Kupcinskas L, et al. Once-daily budesonide MMX in active, mild-to-moderate ulcerative colitis: results from the randomised CORE II study. *Gut*. 2014;63(3):433–441. doi:10.1136/gutjnl-2012-304258
- Zhang Y, Han D, Yu S, et al. Protective effect of iridoid glycosides of the leaves of *Syringa oblata* Lindl. on dextran sulfate sodium-induced ulcerative colitis by inhibition of the TLR2/4/MyD88/NF- $\kappa$ B Signaling Pathway. *Biomed Res Int*. 2020;2020:7650123.
- Frank DN, St Amand AL, Feldman RA, Boedeker EC, Harpaz N, Pace NR. Molecular-phylogenetic characterization of microbial community imbalances in human inflammatory bowel diseases. *Proc Natl Acad Sci U S A*. 2007;104(34):13780–13785. doi:10.1073/pnas.0706625104
- Liu X, Wang J. Anti-inflammatory effects of iridoid glycosides fraction of *Folium syringae* leaves on TNBS-induced colitis in rats. *J Ethnopharmacol*. 2011;133(2):780–787. doi:10.1016/j.jep.2010.11.010
- Lamprecht A. IBD: selective nanoparticle adhesion can enhance colitis therapy. *Nat Rev Gastroenterology Hepatology*. 2010;7(6):311–312. doi:10.1038/nrgastro.2010.66
- Lautenschläger C, Schmidt C, Fischer D, Stallmach A. Drug delivery strategies in the therapy of inflammatory bowel disease. *Adv Drug Deliv Rev*. 2014;71:58–76. doi:10.1016/j.addr.2013.10.001
- Liu -Y-Y, Chen X-R, Gao L-F, et al. Spectrum-effect relationships between the bioactive ingredient of *Syringa oblata* Lindl. leaves and its role in inhibiting the biofilm formation of streptococcus suis. *Front Pharmacol*. 2018;9:570. doi:10.3389/fphar.2018.00570
- Wang DD, Liu SQ, Chen YJ, Wu LJ, Sun JY, Zhu TR. [Studies on the active constituents of *Syringa oblata* Lindl]. *Yao Xue Xue Bao*. 1982;17(12):951–954.
- Liu X, Wang JM, Bereswill S. Iridoid Glycosides Fraction of *Folium syringae* Leaves Modulates NF- $\kappa$ B Signal Pathway and Intestinal Epithelial Cells Apoptosis in Experimental Colitis. *PLoS One*. 2011;6(9):e24740. doi:10.1371/journal.pone.0024740
- Guan Q, Sun S, Li X, et al. Preparation, in vitro and in vivo evaluation of mPEG-PLGA nanoparticles co-loaded with syringopicroside and hydroxytyrosol. *J Mater Sci Mater Med*. 2016;27(2):24. doi:10.1007/s10856-015-5641-x
- Naeem M, Choi M, Cao J, et al. Colon-targeted delivery of budesonide using dual pH- and time-dependent polymeric nanoparticles for colitis therapy. *Drug Des Devel Ther*. 2015;9:3789–3799. doi:10.2147/DDDT.S88672
- El-Maghawry E, Tadros MI, Elkheshen SA, Abd-Elbary A. Eudragit (®)-S100 Coated PLGA Nanoparticles for Colon Targeting of Etoricoxib: optimization and Pharmacokinetic Assessments in Healthy Human Volunteers. *Int J Nanomedicine*. 2020;15:3965–3980. doi:10.2147/IJN.S244124
- Naeem M, Bae J, Oshi MA, et al. Colon-targeted delivery of cyclosporine A using dual-functional Eudragit(®) FS30D/PLGA nanoparticles ameliorates murine experimental colitis. *Int J Nanomedicine*. 2018;13:1225–1240. doi:10.2147/IJN.S157566
- Wang QS, Wang GF, Zhou J, Gao LN, Cui YL. Colon targeted oral drug delivery system based on alginate-chitosan microspheres loaded with icariin in the treatment of ulcerative colitis. *Int J Pharm*. 2016;515(1–2):176–185. doi:10.1016/j.ijpharm.2016.10.002
- Brusini R, Varna M, Couvreur P. Advanced nanomedicines for the treatment of inflammatory diseases. *Adv Drug Deliv Rev*. 2020;157:161–178. doi:10.1016/j.addr.2020.07.010
- Youshia J, Lamprecht A. Size-dependent nanoparticulate drug delivery in inflammatory bowel diseases. *Expert Opin Drug Deliv*. 2016;13(2):281–294. doi:10.1517/17425247.2016.1114604
- Wu P, Zhou Q, Zhu H, Zhuang Y, Bao J. Enhanced antitumor efficacy in colon cancer using EGF functionalized PLGA nanoparticles loaded with 5-Fluorouracil and perfluorocarbon. *BMC Cancer*. 2020;20(1):354. doi:10.1186/s12885-020-06803-7
- Shokoohinia P, Hajialyani M, Sadrjavadi K, et al. Microfluidic-assisted preparation of PLGA nanoparticles for drug delivery purposes: experimental study and computational fluid dynamic simulation. *Res Pharm Sci*. 2019;14(5):459–470. doi:10.4103/1735-5362.268207
- Kuang C, Sun Y, Li B, et al. Preparation and evaluation of duloxetine hydrochloride enteric-coated pellets with different enteric polymers. *Asian J Pharm Sci*. 2017;12(3):216–226. doi:10.1016/j.ajps.2016.08.007
- Kumari A, Jain A, Hurkat P, Tiwari A, Jain SK. Eudragit S100 coated microspheres for Colon targeting of prednisolone. *Drug Dev Ind Pharm*. 2018;44(6):902–913. doi:10.1080/03639045.2017.1420079
- Fude C, Lei Y, Jie J, Hongze P, Wenhui L, Dongmei C. Preparation and in vitro evaluation of pH, time-based and enzyme-degradable pellets for colonic drug delivery. *Drug Dev Ind Pharm*. 2007;33(9):999–1007. doi:10.1080/03639040601150393
- Ansari M, Sadarani B, Majumdar A. Colon targeted beads loaded with pterostilbene: formulation, optimization, characterization and in vivo evaluation. *Saudi Pharm j*. 2019;27:71–81. doi:10.1016/j.jsps.2018.07.021
- Mennini N, Furlanetto S, Cirri M, Mura P. Quality by design approach for developing chitosan-Ca-alginate microspheres for colon delivery of celecoxib-hydroxypropyl- $\beta$ -cyclodextrin-PVP complex. *Eur j Pharm Biopharm*. 2012;80(1):67–75. doi:10.1016/j.ejpb.2011.08.002
- Frieder J, Kivelevitch D, Haugh I, Watson I, Menter A. Anti-IL-23 and Anti-IL-17 Biologic Agents for the Treatment of Immune-Mediated Inflammatory Conditions. *Clin Pharmacol Ther*. 2018;103(1):88–101. doi:10.1002/cpt.893
- Lin X, Li J, Zhao Q, Feng JR, Gao Q, Nie JY. WGCNA Reveals Key Roles of IL8 and MMP-9 in Progression of Involvement Area in Colon of Patients with Ulcerative Colitis. *Curr Med Sci*. 2018;38:252–258. doi:10.1007/s11596-018-1873-6

26. Stenke E, Bourke B, Knaus UG. Correction to: NADPH Oxidases in Inflammatory Bowel Disease. *Methods Mol Biol.* 2019;1982: C1.
27. Takeuchi K, Amagase K. Roles of Cyclooxygenase, Prostaglandin E2 and EP Receptors in Mucosal Protection and Ulcer Healing in the Gastrointestinal Tract. *Curr Pharm Des.* 2018;24(18):2002–2011. doi:10.2174/1381612824666180629111227
28. Li Y, Dang Y, Han D, et al. An Angiopep-2 functionalized nanoformulation enhances brain accumulation of tanshinone IIA and exerts neuroprotective effects against ischemic stroke. *New J Chem.* 2018;42(21):17359–17370. doi:10.1039/C8NJ02441C
29. Dai C, Zheng CQ, Meng FJ, Zhou Z, Sang LX, Jiang M. VSL#3 probiotics exerts the anti-inflammatory activity via PI3k/Akt and NF- $\kappa$ B pathway in rat model of DSS-induced colitis. *Mol Cell Biochem.* 2013;374(1–2):1–11. doi:10.1007/s11010-012-1488-3
30. Dong S, Chen M, Dai F, et al. 5-Hydroxytryptamine (5-HT)-exacerbated DSS-induced colitis is associated with elevated NADPH oxidase expression in the colon. *J Cell Biochem.* 2019;120(6):9230–9242. doi:10.1002/jcb.28198
31. Zhu Q, Zheng P, Chen X, Zhou F, He Q, Yang Y. Andrographolide presents therapeutic effect on ulcerative colitis through the inhibition of IL-23/IL-17 axis. *Am J Transl Res.* 2018;10:465–473.
32. Li Y, Soendergaard C, Bergenheim FH, et al. COX-2–PGE2 signaling impairs intestinal epithelial regeneration and associates with TNF inhibitor responsiveness in ulcerative colitis. *EBioMedicine.* 2018;36:497–507. doi:10.1016/j.ebiom.2018.08.040
33. Deng S, Tang Q, Duan X, et al. Uncovering the anticancer mechanism of compound Sophorae decoction against ulcerative colitis-related colorectal cancer in mice. *Evid Based Complement Alter Med.* 2019;2019:8128170. doi:10.1155/2019/8128170

## International Journal of Nanomedicine

Dovepress

### Publish your work in this journal

The International Journal of Nanomedicine is an international, peer-reviewed journal focusing on the application of nanotechnology in diagnostics, therapeutics, and drug delivery systems throughout the biomedical field. This journal is indexed on PubMed Central, MedLine, CAS, SciSearch®, Current Contents®/Clinical Medicine,

Journal Citation Reports/Science Edition, EMBase, Scopus and the Elsevier Bibliographic databases. The manuscript management system is completely online and includes a very quick and fair peer-review system, which is all easy to use. Visit <http://www.dovepress.com/testimonials.php> to read real quotes from published authors.

Submit your manuscript here: <https://www.dovepress.com/international-journal-of-nanomedicine-journal>